AIAA-98-0280

NOISE MEASUREMENTS IN SUPERSONIC JETS TREATED WITH THE MACH WAVE ELIMINATION METHOD

Dimitri Papamoschou*and Marco Debiasi †
Department of Mechanical and Aerospace Engineering
University of California, Irvine
Irvine, CA 92697-3975

Abstract

We report noise measurements for perfectly-expanded coaxial jets composed of a supersonic primary stream at velocity of 920 m/s and a coflow stream at conditions designed to prevent formation of Mach waves. The resulting sound field was compared to that emitted by a single jet at the conditions of the primary stream. Overall sound pressure levels (OASPL) and noise spectra were obtained at many radial and azimuthal positions around the jet exit. Equal-thrust comparisons were made by using geometric scaling. At equal thrust, Mach wave elimination reduced the near-field OASPL by 11 dB and the far-field OASPL by 5 dB. The mid-to-high frequency region of the spectrum, which is most pertinent to aircraft noise, was reduced by 20 dB in the near field and by 9 dB in the far field. It is demonstrated that Mach waves account for at least 85% of the sound field most relevant to aircraft noise.

I. Introduction

Mach wave radiation is an integral feature of jets with velocity in excess of about 450 m/s. It is caused by the supersonic convection of turbulent eddies in the proximity of the jet exit. Because it is relevant to the take-off noise of supersonic aircraft, it has been the subject of numerous experimental [1, 2] and theoretical [3, 4, 5] works. Photographic evidence, directivity of the measured sound, and analytical/computational results suggest that Mach waves constitute an important source of noise in supersonic jets.

However, there have been few attempts to distinguish between Mach wave emission and other sources of noise, namely shock-induced noise (screech and broadband) in imperfectly expanded jets and "conventional" quadrupole noise. While shock noise can be eliminated by perfect expansion of the jet, separating Mach wave emission from quadrupole noise is very difficult. The same feature responsible for Mach wave emission, high velocity, also produces strong quadrupole sources, particularly in the region downstream of the potential core where large eddies form. One notable work that attempted to distinguish between these two sources of sound is by Bishop et al. [6], where a sound absorbing screen with a hole was used to separate sources of noise located downstream of the potential core from those located upstream of it. The authors concluded that Mach wave radiation accounts for as much as 20 dB of the total noise field. We consider this conclusion flawed because their jet was highly underexpanded, thus emitted substantial screech noise which the screen undoubtedly suppressed. Futhermore, the authors assumed that all of the upstream noise consisted of Mach wave radiation without providing full justification. At this stage of our understanding of jet noise, the fraction of noise attributable to Mach waves, especially in the far field, is not known. Moreover, some works suggested that the frequency of Mach waves is too high to be of significance to aircraft noise [7].

Recently, it was demonstrated that Mach waves can be eliminated by addition of an annular coflow around the primary jet such that the primary eddies become subsonic with respect to the coflow and the coflow eddies are subsonic with respect to the ambient [8]. An empirical model for the eddy convective velocity U_c, based on its direct measurement in shear layers [9], was used to predict the appropriate conditions of the coflow in terms of its temperature and Mach number. (see Fig. 2). The model is complex, but a rough approximation would be that eddies of the inner shear layer propagate with 80% of the jet velocity and those of the outer shear layer with 70% of the coflow velocity. The method, called Mach Wave Elimination (MWE), prevents formation of Mach waves without entailing mechanical suppressors. In an engine, the coflow could be supplied by the fan stream or by an ejector. Fundamental studies of the noise characteristics of coaxial

*Associate Professor, member AIAA
†Graduate Student, member AIAA
0

high-speed jets have been scarce. Experimental studies were confined to either subsonic Mach numbers [10] or underexpanded cold supersonic jets [11]. A recent, highly detailed theoretical study by Dahl & Morris [12] illuminates the effects of instability waves on the radiated sound field but did not encompass Mach wave elimination conditions.

Evidence of Mach wave elimination has so far been based on schlieren photography. The present study evaluates the MWE using microphone surveys of the sound emitted by a high-speed, low-density jet. It also sheds some light on the questions raised above, i.e., what fraction of the emitted sound is due to Mach waves and which portion of the frequency spectrum they affect.

III. Flow Apparatus

Experiments were conducted in a coaxial jet facility described in detail in [8]. Mixtures of helium and air were supplied to a concentric nozzle arrangement shown in Fig. 1. The inner nozzle, of 12.7-mm exit diameter, was designed by the method of characteristics for Mach number $M_1 = 1.5$. The outer nozzle formed a smooth contraction terminating in an exit diameter of 25.4 mm. Precisely-metered mixtures of helium and

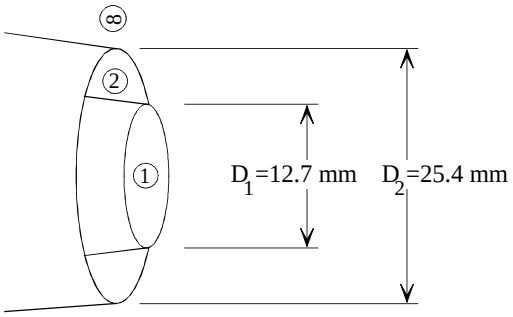

Figure 1: Coaxial jet geometry.

air were supplied to the nozzles, which exhausted into ambient, still air. The total pressure of the inner (primary) flow was set at 375 kPa, resulting in a pressure-matched jet. Special care was taken to maintain that total pressure to within 1% of the pressure-matched value. For the majority of the experiments described here, the outer (coflow) stream was supplied at a total pressure of 160 kPa, resulting in an exit Mach number $M_2 = 0.83$. Helium-air mixtures duplicate very accurately the density, velocity, and speed of sound of a heated jet. By regulating the mass fractions of helium and air, thereby regulating the gas constant of the mixture, we controlled the jet velocity at fixed Mach number. The density of the mixture can be translated to the effective temperature of a heated jet via the relation $\rho_\infty/\rho = T/T_\infty$, where ∞ refers to the ambient conditions. Our baseline case has a jet velocity $U_1 = 920$ m/s, which is typical of supersonic engines. The automated facility was instrumented with pressure transducers (Setra Model 280) recording the total pressures in the primary and coflow streams as well as the centerline pitot pressure. A schlieren system, illuminated by a 20-ns spark gap (Xenon Nanolamp), enabled frozen visualization of the flow.

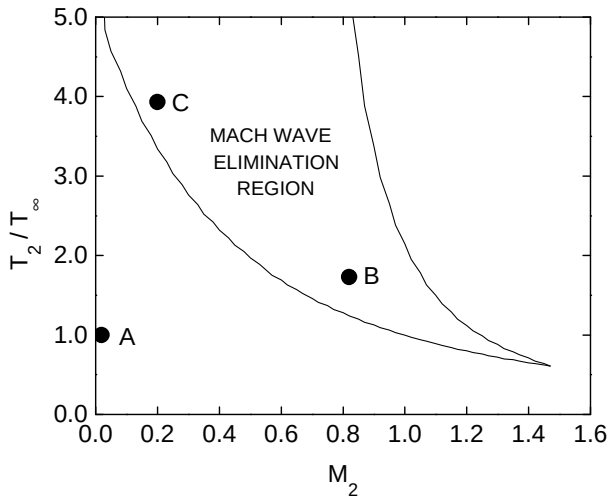

Figure 2: Mach wave elimination region for a jet with $M_1 = 1.5$ and $T_1/T_\infty = 2.8$. Location of Cases A, B, and C is indicated.

The table below summarizes the flow conditions covered in this paper. Cases A and B comprise the majority of the experiments, while Cases C and D represent limited investigations to obtain important reference data. Figure 2 shows the location of Cases A, B and C on the Mach wave elimination diagram.

Table 1. Flow Conditions

Case	M_1	U_1	$\frac{T_1}{T_\infty}$	M_2	U_2	$\frac{T_2}{T_\infty}$	$\frac{\dot{m}_2}{\dot{m}_1}$	$\frac{F_{1+2}}{F_1}$
A	1.5	920	2.8	0.00	0	1.0	0	1.00
B	1.5	920	2.8	0.83	415	1.7	2.1	1.92
C	1.5	920	2.8	0.15	120	4.0	2.0	1.15
D	1.5	700	1.7	0.00	0	1.0	0	1.00

U in m/s, T denotes effective temperature

The last column indicates the calculated ratio of the thrust of the combined flow over the thrust of the primary flow. The Reynolds number of the primary jet, based in D_1, was 380,000 for Cases A, B, and C, and 490,000 for Case D.

IV. Sound Measurement

Data Collection

The jet noise was recorded by a one-eighth inch condenser microphone connected to a preamplifier and power supply (Bruel & Kjaer Models 4138, 2670, and 5935L, respectively). The microphone has a frequency response up to 150 kHz and was sampled at 400 kHz by a fast analog-to-digital board (National Instruments AT-MIO-16E1) installed in a Pentium Pro computer. Each recording consisted of 54280 samples (135 ms), corresponding to passage of about 10,000 eddies the size of the inner-jet diameter. Occasionally, the sample size was increased to 131072 but there was no significant difference seen in the results. The signal was high-pass filtered at 500 Hz by a Butterworth filter to remove spurious low-frequency noise. The power spectrum of each recording was computed using a 512-point FFT with full Hanning window. The microphone was calibrated daily before each series of recordings (Bruel & Kjaer Model 4231 calibrator).

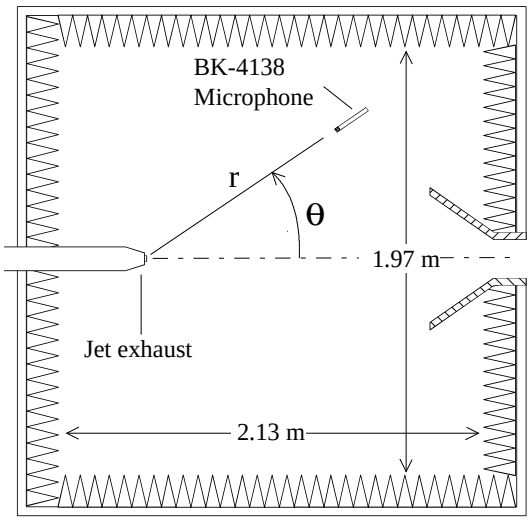

Figure 3: Anechoic chamber and positioning of jet and microphone.

Sound measurements were conducted inside an anechoic chamber, approximately 8-m^3 in internal size, lined with acoustic wedges (Sonex) with an absorption coefficient higher than 1.0 for frequencies above 500 Hz. Figure 3 provides a cutaway of the chamber and shows the jet and microphone positions. The microphone was mounted on an arm which pivoted around an axis passing through the center of the jet exit. This arrangement enabled sound measurement at a variety of radial (r) and azimuthal (θ) positions, r ranging from 0.038 to 1.52 m and θ ranging from 20^o to 100^o, measured counter-clockwise from the jet axis. For very large distances, the range of azimuthal positions was limited due to interference with the chamber's walls.

Data Processing

Signal processing yielded two important noise parameters, the overall sound pressure level (OASPL) which describes the total noise at a given point and the sound pressure level (SPL) spectrum which shows the distribution of noise versus frequency. The units for both quantities are decibels (dB). The OASPL is defined as

$$\text{OASPL} = 20 \log_{10}\left(\frac{p'_{\text{rms}}}{p_{\text{ref}}}\right) \quad (1)$$

where p'_{rms} is the root mean square pressure fluctuation and $p_{\text{ref}} = 20$ μPa is the commonly used reference pressure. Alternatively, the OASPL can be computed in the frequency domain by

$$\text{OASPL} = 10 \log_{10} \int_0^\infty S(f) df \quad (2)$$

where $S(f)$ is the properly-normalized power spectrum of p'/p_{ref}. The SPL spectrum is given by

$$\text{SPL}(f) = 10 \log_{10} S(f) \quad (3)$$

Before calculating these quantities, the microphone signal must be corrected for the frequency response and the free-field response. Both corrections are done in the frequency domain according to data provided by the microphone manufacturer (Bruel & Kjaer). While the frequency-response correction is minor, the free-field response correction can be significant for $f > 50$ kHz. The free-field correction depends on the frequency f and the angle ϕ between the sound propagation vector and the microphone axis. It is a consequence of the sound wavelength becoming of the same order as the microphone diameter. Because it is an important correction, we independently verified the Bruel & Kjaer correction curves for ϕ=0^o and 90^o by changing the microphone incidence angle in the far field, where the sound propagation vector is in the radial direction. For the near-field ($r/D_1 < 12$) we assumed that sound propagates normal to the Mach waves, which we visualized, except for $\theta > 60^o$ where Mach waves do not exist and where propagation is assumed to be radial.

Another complication of working at very high frequencies is atmospheric absorption of sound. For given temperature, pressure, and humidity, absorption increases with f^2, so it has much larger impact on subscale tests than on full-size tests. In our experiments,

absorption of the 100-kHz component of noise ranges from 2 to 4 dB/m depending on the relative humidity [13]. Absorption should not affect the SPL comparisons at given frequency, but is expected to have a small effect on the OASPL comparisons by producing a larger attenuation of OASPL in cases with larger high-frequency content. We have not attempted to account for the effect of absorption on our measurements.

For each measurement location, the power spectrum was computed according to

$$S(f) = S_{\mathrm{raw}}(f) + \Delta S_{\mathrm{fr}}(f) + \Delta S_{\mathrm{ff}}(f,\phi) \qquad (4)$$

where $S_{\mathrm{raw}}(f)$ is the raw spectrum, $\Delta S_{\mathrm{fr}}(f)$ is the frequency-response correction and $\Delta S_{\mathrm{ff}}(f,\phi)$ is the free-field correction. The SPL spectrum was then computed according to Eq. 3 and the OASPL according to Eq. 2, with the limits of integration from 0.5 to 150 kHz. The difference in OASPL computed using Eq. 1 (with the uncorrected p'_{rms}) from that given by Eq. 2 is at most 2 dB.

Equal Thrust Scaling

Application of the Mach wave elimination technique is accompanied by an increase in thrust and attendant introduction of new sources of sound. Due to the complex interaction of the coflow with the primary jet, the effect of the coflow on the noise field is not additive. To assess the full impact of Mach wave elimination, it is important to compare flows at equal thrust while preserving the physics of the problem. To this end, we used simple geometric scaling and maintained constant the velocity, density, and Mach number. With these parameters fixed, the sound intensity (p'^2) at a given radial and azimuthal position scales directly with D^2 [14] and so does the thrust. For constant thrust, we compared the untreated jet with the treated jet scaled down (in diameter) by the square root of the thrust ratio F_{1+2}/F_1. The sound intensity of the treated jet is thus divided by F_{1+2}/F_1 and the resulting correction in terms of SPL is

$$\Delta\mathrm{SPL} = -10 \log_{10}\left(\frac{F_{1+2}}{F_1}\right)$$

For a thrust ratio of 1.92 (Case B), the correction is -2.8 dB. The same correction applies to the OASPL data. It is important to note that this thrust correction is based solely on noise data that we measured; no assumptions, such as a power-law dependence of sound intensity on velocity, are involved.

(A)

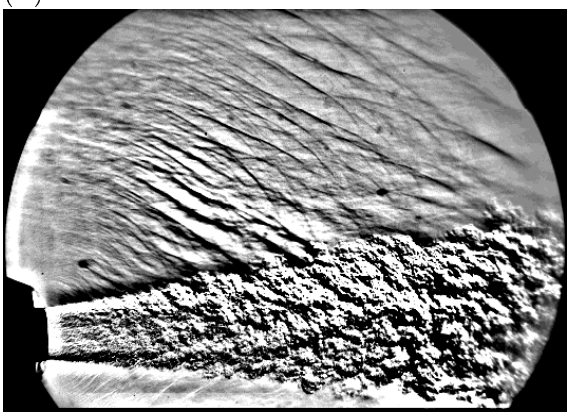

(B)

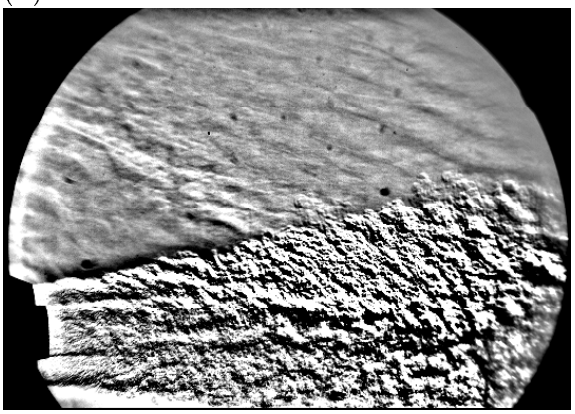

Figure 4: Schlieren visualizations of Cases A and B.

V. Global Features of the Jet

Figure 4 shows schlieren images of the jets of Cases A and B. For the untreated jet (Case A), the Mach waves are inclined at a slope of approximately 30^o, from which we infer that eddies travel with Mach number 2.0, and velocity of 700 m/s, with respect to the ambient. The propagation vector of the Mach waves is thus inclined at 60^o with respect to the jet axis. Application of the coflow (Case B) eliminates the Mach waves from the visible field. Both Cases A and B have a substantial growth rate, an effect of the low density (high effective temperature) of the jet. Cold jets, on the other and, spread very slowly, thus are unrepresentative of the exhaust of an engine.

Figure 5 shows the centerline Mach number distributions for Cases A and B, inferred from pitot measurements. The coflow has small impact on the Mach number decay versus axial distance. The potential core ends within $x/D_1 = 6$, which is approximately one half of the field of view of the images presented here. It is notable that significant Mach waves are generated past the potential core.

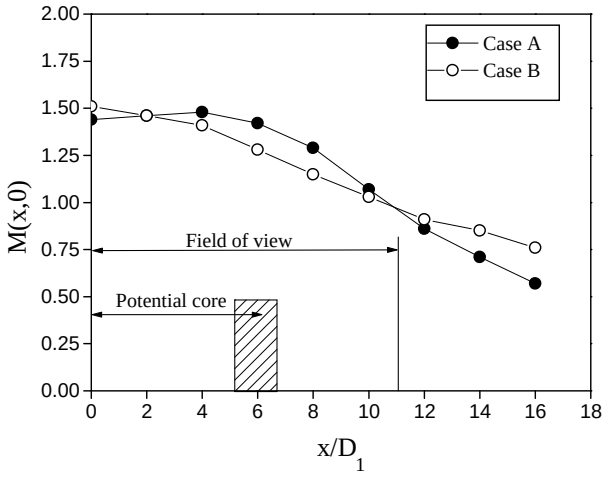

Figure 5: Centerline Mach number distributions for Cases A and B.

VI. Noise Characteristics

Cases A and B

We begin our discussion with the SPL spectra at the peak directivity angle and at various radial locations. Figure 6(a) shows the very-near field spectrum at $r/D_1 = 3$. The untreated jet has a very flat spectrum, indicating equal contribution of large and small scales towards noise generation. Application of treatment suppresses dramatically the middle and high-frequency components of the spectrum while there is an increase of the very low frequency components. That increase is due to the proximity (within a few millimeters) of the microphone to the edge of the coflow. The SPL reduction at $St = 1.0$ is 18 dB (21 dB at equal thrust). As we move the microphone away to $r/D_1 = 6.0$ (Fig. 6(b)), treatment produces a small increase at the very low frequencies and a reduction of about 14 dB (17 dB at equal thrust) at the higher frequencies. The OASPL reduction is 8 dB (11 dB at equal thrust). Figure 6(c) depicts the far-field spectra at $r/D_1 = 120$. Treatment reduces the high-frequency components by about 6 dB (9 dB at equal thrust) while the very-low frequency components remain basically unchanged. The reduction in OASPL is 2 dB (5 dB at equal thrust). The spectrum peaks at a very low Strouhal number of about 0.15 ($f = 10$ kHz), which is indicative of low-velocity, large-scale disturbances unrelated to supersonic eddies. It is important to realize that the low-frequency part of the spectrum, $0 < St < 0.25$, is insignificant for full-scale engine noise, a point we will discuss further at the end of this section.

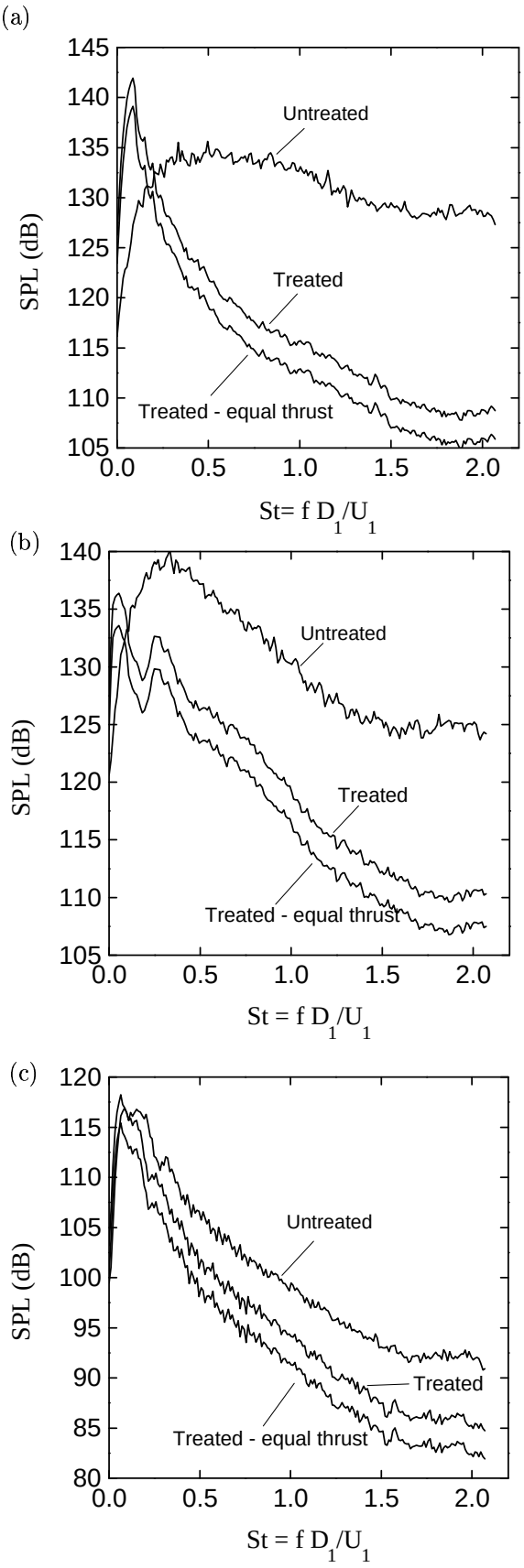

Figure 6: Sound pressure level spectra of Cases A and B at the peak directivity angle; (a) $r/D_1 = 3$, $\theta = 40^o$; (b) $r/D_1 = 6$, $\theta = 30^o$; (c) $r/D_1 = 120$, $\theta = 50^o$.

Next we examine the variation of OASPL with radial and azimuthal position for Cases A and B, depicted in Figs. 7(a) and (b). The untreated and treated flows share the same trends: at small distances, OASPL peaks at low angles while at large distances it peaks at $\theta = 50^o$. While this is close to the Mach wave propagation direction of 60^o, it would also be consistent with the directivity of a low-speed jet [14]. In other words, it is not clear that the far-field directivity of the OASPL is due to Mach wave emission alone. To further elucidate this point, we plot the directivity of the spectrum range $1.2 < St < 1.6$, shown in Figs. 8(a) and (b). For the untreated case, the far-field directivity peaks at 60^o, consistent with the direction of the Mach waves. For the treated case, that peak is greatly suppressed, consistent with elimination of most, if not all, of the Mach waves.

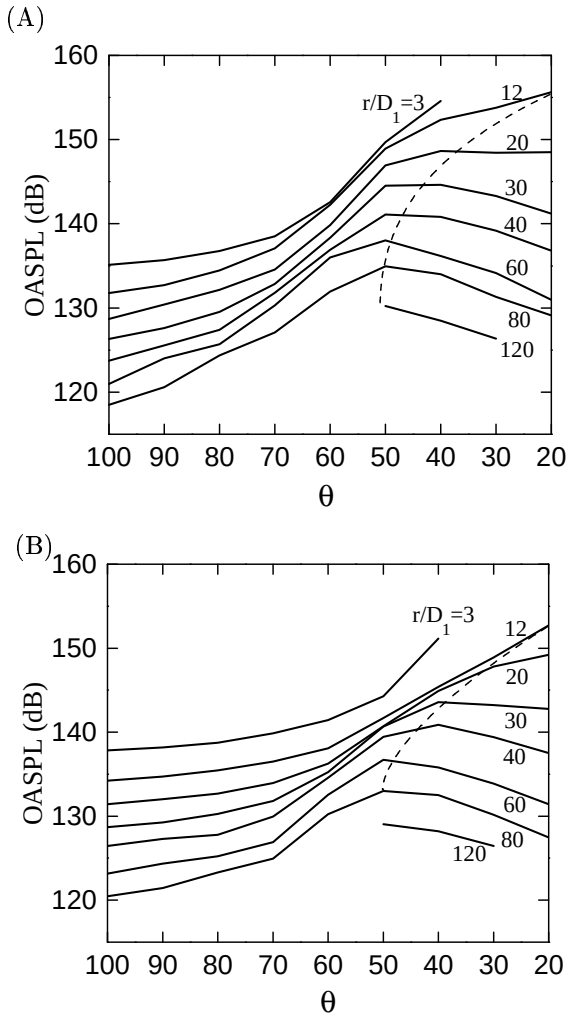

Figure 7: OASPL versus r and θ for Cases A and B. Dashed line indicates approximate trend of peak OASPL.

These findings, together with the spectra of Fig. 6(c), indicate that Mach waves constitute a significant component of the far-field noise at Strouhal numbers larger than about 0.5.

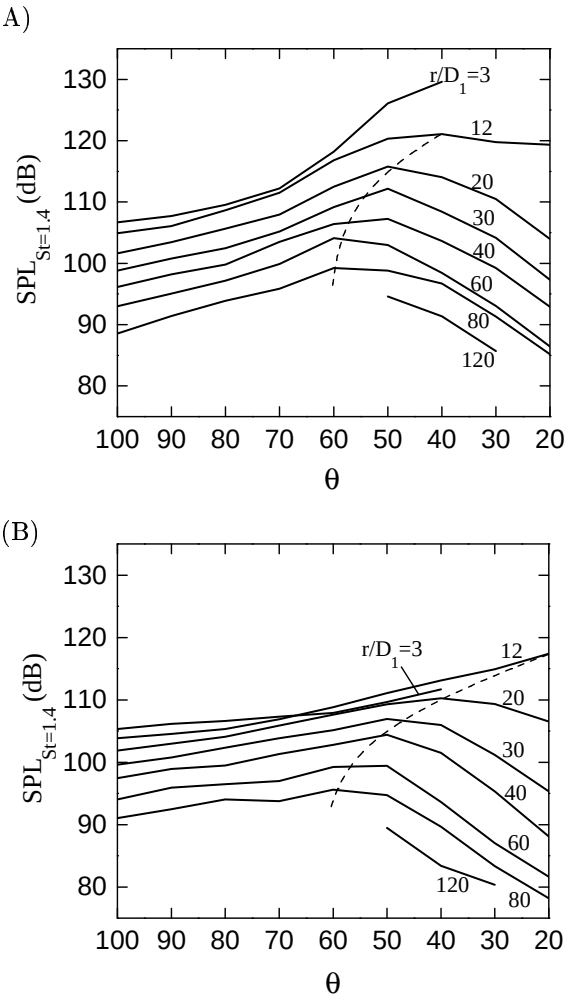

Figure 8: High-frequency component of spectrum plotted versus r and θ for Cases A and B. Dashed line indicates approximate trend of peak SPL.

The Strouhal number corresponding to the peak value of the SPL spectrum, $St_{\max}$, is plotted versus r and θ, in Figs. 9 (a) and (b). For the untreated jet, the overall trend is a decrease in $St_{\max}$ with increasing r and decreasing θ, with exception of the near field ($r/D_1 = 3$) where $St_{\max}$ becomes large at small θ, consistent with high-frequency, intense Mach wave emission close to the jet. Elimination of Mach waves changes this near-field trend dramatically, rendering it similar to the far-field trend noted above. There is an appreciable overall decrease in $St_{\max}$ when treatment is applied.

Identification of the far field is a concern for any jet noise experiment. The far field is supposed to be far away from all the sources of noise [14]. In the far field, the pressure fluctuation along a given azimuthal direction should decay with distance according to $p'_{\rm rms} \sim 1/r$, or $p'_{\rm rms} r$ =constant. To test this

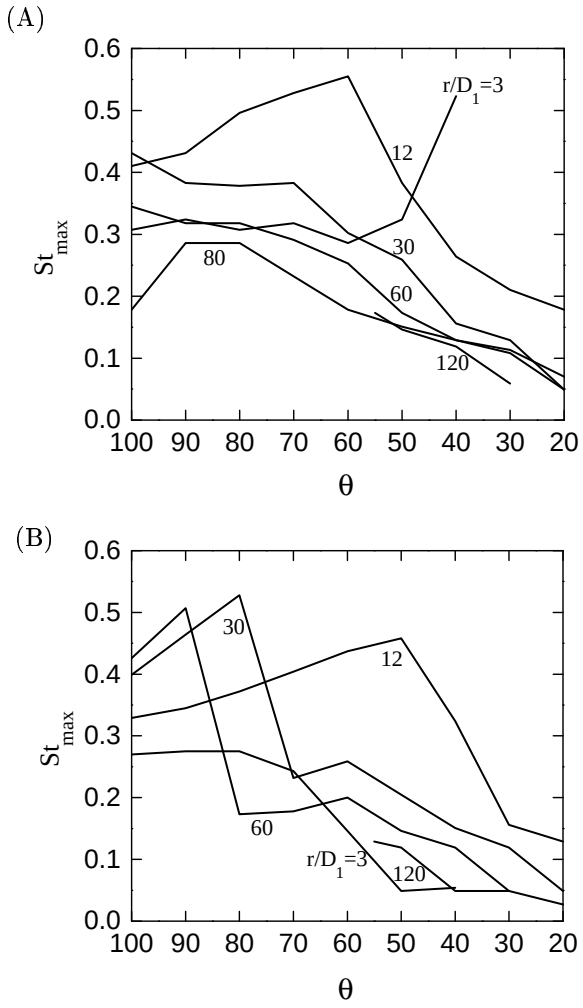

Figure 9: Strouhal number at spectrum peak versus r and θ for Cases A and B.

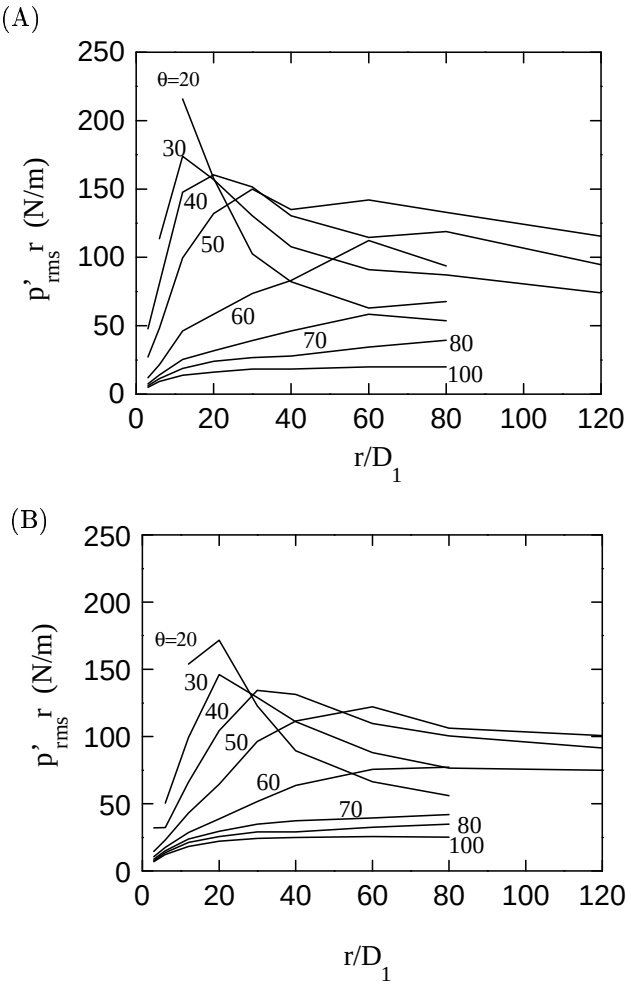

Figure 10: The product $p'_{\rm rms}r$ versus r and θ for Cases A and B.

relation, we plot $p'_{\rm rms}r$ versus r and θ in Figs. 10(a) and (b). For both the treated and untreated cases, it reaches nearly-constant values for $r/D_1 > 60$. The small decay of Case A for $r/D_1 > 80$ may be due to sound absorption, which is expected to impact Case A more than Case B (see related discussion in Section IV). We are thus confident that the surveys done at $r/D_1 = 80$ and 120 are indeed in the far field. Note that there is significant addition of noise sources, indicated by an increase in $p'_{\rm rms}r$, up to $r/D_1 = 40$!

Cases C and D

Addition of the coflow to the primary jet alters the fluid dynamics of the situation, particularly when the coflow has a substantial momentum flux, as in Case B. This in turn changes the distribution and strength of the quadrupole sources of noise, an effect that may interfere with the effect of Mach wave elimination. In an effort to isolate the impact of Mach wave elimination, we tested Case C which has a coflow at very low velocity and high speed of sound, supplied by a large nozzle ($D_2/D_1 = 4.0$). Here the coflow has very low momentum flux, so it should not alter the fluid dynamics of the jet–besides eliminating the Mach waves. The far-field spectrum of Case C is compared with that of the untreated jet (Case A) in Fig. 11. Equal-thrust correction is very small here (0.5 dB), so it is omitted. There is noise reduction across the entire spectrum. The high-frequency part of the spectrum is reduced by about 9 dB, which is roughly the same reduction achieved in Case B with equal-thrust scaling (Fig. 6 (d)). This indicates that most, if not all, of the high-frequency noise reduction in Case B resulted from elimination of Mach waves. Case C provides strong evidence that Mach waves constitute the dominant source of noise at the higher end of the spectrum which, as we will examine below, is most relevant to aircraft noise. In terms of sound intensity, the contribution of Mach waves is at least 85% of the total sound field at those frequencies.

In several engine designs, the coflow (fan) and primary

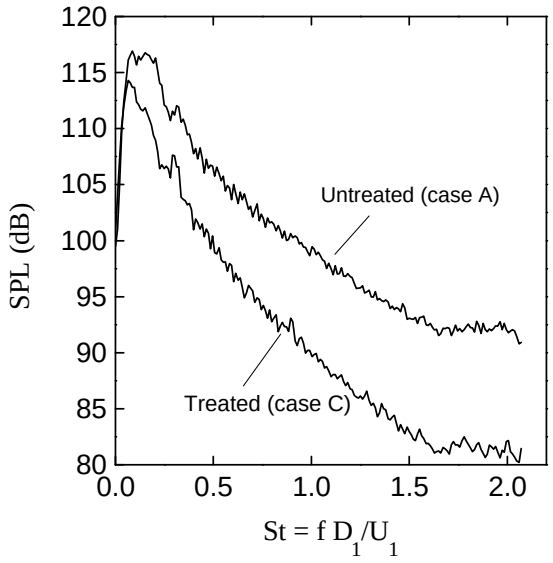

Figure 11: Spectra at $r/D_1 = 120$ and $\theta = 50^o$ for Cases A and C.

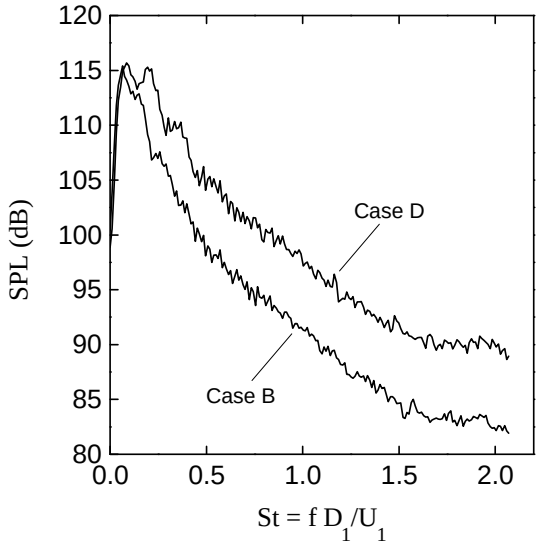

Figure 12: Spectra at $r/D_1 = 120$ and $\theta = 50^o$ for unmixed coaxial jet (Case B) and fully-mixed single jet (Case D).

(core) streams are mixed before exhausting from the nozzle. We felt that it was important from a propulsive viewpoint (not so much a physical viewpoint) to examine the noise characteristics of a "fully mixed" jet. A thermodynamic calculation shows that mixing the primary and coflow streams of Case B, and expanding them through a single Mach 1.5 nozzle, yields an exit velocity U_1=700 m/s and effective temperature $T_1/T_\infty = 1.7$. We simulated this jet, Case D, by increasing the mass fraction of air in the helium-air mixture and expanding the mixture through our Mach 1.5 nozzle. Due to its lower velocity, Case D has weaker Mach wave emission than Case A, hence the physics of the problem are now different. The equal-thrust comparison of Cases D and B is shown in Fig. 12, where it is seen that the "unmixed" Case B has a substantial benefit, about 7 dB at the high frequencies, over the "fully mixed" Case D. This suggests that an unmixed core-fan exhaust at MWE conditions will be beneficial compared to a mixed exhaust. One should also keep in mind that high-speed mixing produces significant thrust losses, not just from the drag of the mechanical devices but also from the total pressure loss due to mixing itself [15].

Impact on Aircraft Noise

The relevance of noise measurements cannot be fully assessed without incorporating the human perception of sound. For aircraft noise, this is commonly done using the Perceived Noise Level (PNL) metric. The small scale of our experiments (about 1/80-scale) prevents us from computing the PNL because our frequencies, scaled to a full-size engine, range only up to 2500 Hz whereas the PNL calculation requires the full audible range up to 20 kHz. Instead, we use the simpler dBA metric which incorporates the same essential features of PNL. First, we divided our frequencies by the scaling factor of 80 in order to scale up our results to a jet diameter $D_1 = 1$ m. Then, we computed the 1/3-octave spectrum and added the dBA correction to it. The resulting far-field spectra for Cases A and B are shown in Fig. 13. They peak at about 1000 Hz, which corresponds to $St = 1.0$, i.e., the portion of the spectrum heavily influenced by Mach waves. For equal thrust, the treated flow provides a noise reduction of about 9 dBA at 1000 Hz. This indicates that Mach waves affect strongly the sensitive part of the noise spectrum.

VII. Conclusions

Noise surveys of Mach 1.5 jets with coflow at Mach wave elimination conditions have been performed. Elimination of Mach waves from a jet with velocity of 920 m/s leads to a dramatic reduction of the near-field noise (about 11 dB OASPL, 20 dB at middle and high frequencies) and an appreciable reduction of the far-field noise (about 5 dB OASPL, 9 dB at frequencies most relevant to aircraft noise). Our measurements suggest that, in a full-scale engine, Mach waves would constitute at least 85% (9 dB) of the sound field to which the human ear is most sensitive. The directivity of the OASPL is in fair, but not very good, agreement

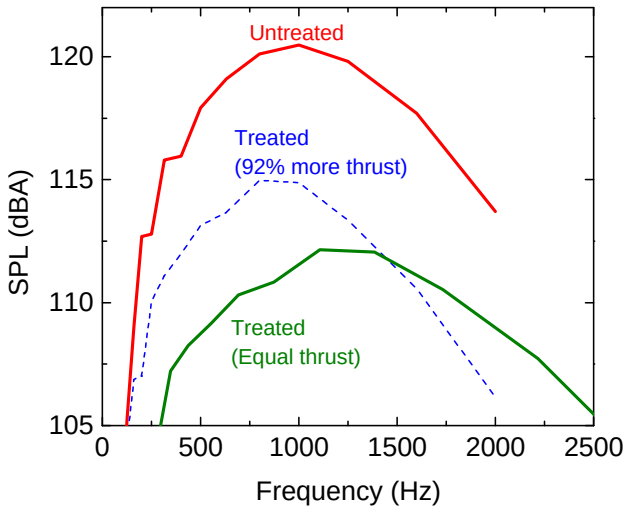

Figure 13: A-weighted, 1/3-octave spectra for Cases A and B, scaled to a full-size engine.

with the propagation direction of Mach waves as visualized in schlieren pictures. In contrast, the directivity of the high-frequency part of the spectrum is in excellent agreement with the visualized propagation of the Mach waves. The ummixed combination of jet and coflow is quieter than their fully-mixed combination exhausting at the Mach number of the jet.

Acknowledgments

The support by NASA Lewis Research Center is gratefully acknowledged (Grant NAG-3-1981 monitored by Dr. Milo Dahl). We thank Ms. Erina Murakami for her assistance with the data acquisition and control part of the experiment.

References

[1] McLaughlin, D.K., Morrison, G.D., and Troutt, T.R., "Experiments on the Instability Waves in a Supersonic Jet and their Acoustic Radiation." *Journal of Fluid Mechanics*, Vol. 69, No. 11, 1975, pp.73-95.

[2] Troutt, T.R., and McLaughlin, D.K., 'Experiments on the Flow and Acoustic Properties of a Moderate Reynolds Number Supersonic Jet.", *Journal of Fluid Mechanics*, Vol. 116, March 1982, pp. 123-156.

[3] Tam, C.K.W. and Burton, D.E., "Sound Generated By Instability Waves of Supersonic Flows. Part 2. Axisymmetric Jets.", *Journal of Fluid Mechanics*, Vol. 138, January 1984, pp.249-271.

[4] Seiner, J.M., Bhat, T.R.S, and Ponton, M.K., "Mach Wave Emission from a High-Temperature Supersonic Jet.", *AIAA Journal*, Vol. 32, No. 12, 1994, pp. 2345-2350.

[5] Mitchell, B.E., Lele, S.K., and Moin, P., "Direct Computation of Mach Wave Radiation in an Axisymmetric Supersonic Jet, " *AIAA Journal*, Vol. 35, No. 10, 1994, pp. 1574-1580.

[6] Bishop, K.A., Ffowcs Williams, J.E., and Smith, W. "On the Noise Sources of the Unsuppressed High-Speed Jet, " *Journal of Fluid Mechanics*, Vol. 50, Part 1, 1971, pp. 21-32.

[7] Tam, C.K.W, "On the Noise of Nearly Ideally Expanded Supersonic Jet, " *Journal of Fluid Mechanics*, Vol. 51, Part 1, 1972, pp. 69-96.

[8] Papamoschou. D., "Mach Wave Elimination from Supersonic Jets, " *AIAA Journal*, Vol. 35, No. 10, 1997, pp. 1604-1611.

[9] Papamoschou, D. and Bunyajitradulya, A. "Evolution of Large Eddies in Compressible Shear Layers," *Physics of Fluids,* Vol. 4, No. 3, 1997, pp. 756-765.

[10] Tanna, H.K., "Coannular Jets - Are They Really Quiet and Why?" *Journal of Sound and Vibration*, Vol. 72, No. 1, 1980, pp. 97-118.

[11] Dosanjh, D.S., Yu, J.C., and Abdelhamid, A.N., "Reduction of Noise from Supersonic Jet Flows," *AIAA Journal*, Vol. 9, No. 12, 1971, pp. 2346-2353.

[12] Dahl, M.D. and Morris, P.J., "Noise from Supersonic Coaxial Jets, Part 2: Normal Velocity Profile," *Journal of Sound and Vibration*, Vol. 200, No.5, 1997, pp. 665-699.

[13] Bass, H.E., Sutherland, L.C., Blackstock, D.T., and Hester, D.M., "Atmospheric Absorption of Sound: Further Developments, " *Journal of the Acoustical Society of America,* Vol. 97, No.1, 1995, pp. 680-683

[14] Goldstein, M.E., "Aeroacoustics, " 1st Ed., McGraw Hill, 1976, New York, pp. 38 and 93.

[15] Papamoschou, D. "Entropy Production and Pressure Variation in Confined turbulent Mixing," *AIAA Journal,* Vol. 31, No. 9, 1993, pp. 1643-1650.